Search for high excitation energy structures in ^{90}Zr and ^{208}Pb, via ^{20}Ne inelastic scattering

S. Fortier and S. Gales

Institut de Physique Nucleaire, 91406 Orsay Cedex, France

Sam M. Austin, W. Benenson, G. M. Crawley, C. Djalali,[*] J. H. Lee,
J. van der Plicht,[†] and J. S. Winfield

National Superconducting Cyclotron Laboratory and Department of Physics and Astronomy, Michigan State University,
East Lansing, Michigan 48824

The inelastic scattering of ^{20}Ne on ^{90}Zr and ^{208}Pb has been studied at 500 and 600 MeV incident energies. High statistics spectra were measured at the grazing angle. For each target, spectra at the two incident energies were compared by means of cross correlation analysis. Structures were observed in the inelastic spectra, but they appeared at different excitation energies at the two beam energies and therefore cannot be identified with high-excitation energy states of the target nuclei in contradiction to the results of previous experiments. Rather they arise from the decay of discrete unbound states in the projectile-like nuclei which were excited by a one-nucleon-transfer reaction. In particular, the structures observed in the transfer-evaporation continuum of the ^{20}Ne $+^{208}$Pb spectra appear to be mainly due to neutron emission from known discrete unbound states in ^{21}Ne. A relatively low upper limit is given for the production cross section of multiphonon states in these systems.

I. INTRODUCTION

It is now well established that giant resonances are strongly excited by heavy ion probes.[1,2] These reactions have been shown to provide an appreciable enhancement of the peak-to-continuum ratio over that obtained with light projectiles and thus are suitable probes for the search for higher-lying, previously unknown, giant resonances. In fact, some investigations of the high-lying inelastic excitation continuum in a number of experiments, which involve symmetric as well as strongly asymmetric systems, have revealed the presence of structures which range up to very high excitation energy.[3-5] The main features of these structures, as summarized in Ref. 4, are that their positions are independent of the nature of the projectile and of the incident energy. They have been interpreted in terms of multiphonon excitations of the target nuclei.[4-6]

However, the experimental evidence about the existence of these high-energy resonances has recently been questioned, especially for ^{208}Pb. In fact, the peaks reported in Ref. 3 in the study of the ^{20}Ne $+^{208}$Pb inelastic scattering at 30 MeV/nucleon, carried out with standard solid state telescopes have not been confirmed in a recent reinvestigation[7] of the same reaction, using a magnetic spectrograph. More recently, searches for high-energy resonances in ^{208}Pb, using ^{17}O and ^{32}S beams, have been unsuccessful.[8] In this context, further investigations which involve several systems at different incident energies are clearly necessary.

In this paper, we report on a search for high-excitation energy structures in ^{208}Pb and ^{90}Zr, via inelastic scattering of ^{20}Ne. The experiment was carried out under similar conditions at two different energies, 500 and 600 MeV. Since some of the ambiguities of the previous results could possibly be attributed to poor statistics, a special effort was made to obtain a large number of counts, especially at the grazing angle where the structures are expected to have the largest cross sections.[4]

The experimental conditions and the data obtained in the inelastic channels are reported in Secs. II and III, respectively. Results from one-nucleon-transfer reactions obtained in the same experiment will be given in a forthcoming paper. However, information on the relative cross sections measured for one-neutron and one-proton pick-up reactions on the same target nuclei will be used in the discussion of the transfer-evaporation continuum observed in the inelastic spectra. The interpretation of the results, in the alternative terms of multiphonon excitation or transfer-evaporation processes, are discussed in Sec. III. It is shown that the structures, which are experimentally observed in the high excitation energy part of the inelastic spectra, are mainly due to the particle decay of discrete unbound states of the projectile-like nuclei which were excited by one-nucleon pick-up reactions.

II. EXPERIMENT

The measurements were carried out using the ^{20}Ne beam from the K500 superconducting cyclotron at Michigan State University. The 98.5% enriched ^{90}Zr and 99.9% enriched ^{208}Pb targets were 1.0 and 3.0 mg/cm^2 thick, respectively. The reaction products were analyzed with the S-320 broad range magnetic spectrograph. The momentum range of the spectrograph is sufficiently large that the entire excitation-energy range

of interest could be covered at one magnetic field setting. The emitted particles were detected by the standard focal plane detector system, which consists of two resistive wire position counters, two ionization chambers for the energy loss measurements, and a stopping plastic scintillator which provided both energy and time signals. The start signal for the time of flight measurement was given by a thin plastic film (0.025 mm thick) located at the entrance of the spectrograph. Its efficiency was checked continuously during the experiment by comparison of the time of flight spectra obtained with it and those obtained from the radio frequency signal of the cyclotron. Different species of nuclei were clearly identified without any ambiguities. In particular, inelastic ^{20}Ne events were well separated from the abundant one-neutron-transfer products ^{21}Ne and ^{19}Ne, as shown in Fig. 1, which displays the mass identification spectrum for the neon isotopes.

The ejectile nuclei were focused on the first position counter, and an overall energy resolution $\Delta E / E$ of about 2×10^{-3} was obtained for the elastic peak with the full 1.5° angular aperture of the spectrograph. An additional determination of the incident angle inside this aperture was achieved by means of a position measurement at the second counter, located 32 cm behind the first one. The whole set of data was stored event-by-event on magnetic tapes and processed off line. During the off line analysis, it was possible to obtain three inelastic spectra, which correspond to 0.5° divisions of the angular range.

The calibration of the focal plane was determined for each incident energy and each target nucleus by determining the position of the elastic peak along the 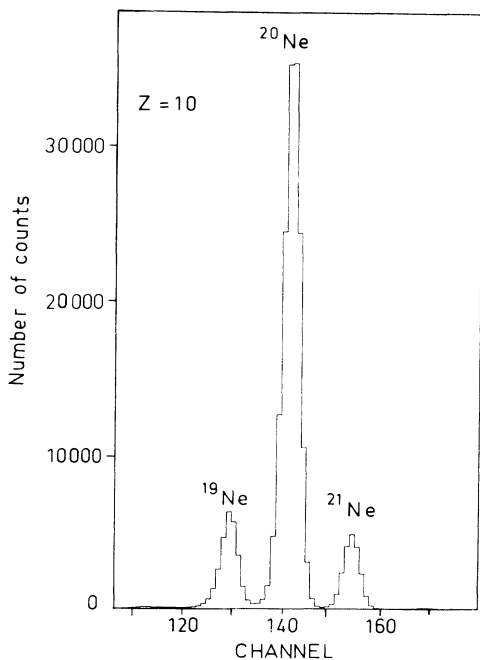counter for different magnetic fields. These independent measurements, carried out at different stages of the experiment, were found to agree in a satisfactory way. The overall accuracy on the excitation energies deduced from this calibration is estimated to be better than 1 MeV, which is adequate for the peaks being investigated in this experiment. During the ^{20}Ne inelastic data taking the elastic scattering counts were suppressed by masking a small part of the detection system with a 5 mm wide metal finger, which was located about one-third of the way down the focal plane. This permitted the observation of an excitation energy range of about 100 and 80 MeV, at 600 and 500 MeV incident energy respectively, and also one-nucleon transfer data by the detection of ^{19}Ne, ^{21}Ne, and ^{21}Na in good conditions.

Data with the best statistics were accumulated at the grazing angle for each reaction, i.e., 5.3° and 6.4° for ^{20}Ne $+ ^{90}$Zr, and 9.5° and 11.5° for ^{20}Ne $+ ^{208}$Pb at 600 and 500 MeV, respectively. At 600 MeV, shorter runs at other forward angles, 7° and 8° for ^{90}Zr and 7°, 11°, 13°, and 15° for ^{208}Pb, were also made in order to observe the angular dependence of the shapes of inelastic spectra at high excitation energy.

If one wants to observe small cross-section fluctuations over a large continuum background, the differential linearity of the detection system has to be well known. For this purpose, spectra at different settings of the spectrograph field were accumulated in an independent way for further comparisons. Two fields were used at 500 MeV incident energy with a shift of about 5 MeV between the two spectra. A slightly different procedure was used for the two experiments at 600 MeV; one-half of the time was spent at one field, and the other half was shared in five fields close to each other with a mutual shift of about 500 keV and an average shift of 6 MeV related to the first one.

In order to compare and add the contributions of runs at different magnetic fields, every momentum spectrum was transformed into an "apparent excitation energy" spectrum with 250 keV energy bins. This scale corresponds to the sum of the excitation energies of the ejectile and residual nuclei in the case of a two-body reaction. The consistency of spectra accumulated at different magnetic fields was further checked by means of a cross-correlation analysis, as reported in Sec. III. A visual examination of the high excitation energy part of the spectra which were obtained with the largest statistical accuracy showed only small defects in the differential linearity. In any case, these defects correspond at worst to a systematic error of about 3% for a 250 keV energy bin. The related upper limits on the production cross sections for possible weak structures, not observed in the presence of a large background, will be estimated in the next section.

III. RESULTS AND DISCUSSION

The inelastic spectra for the two reactions ^{20}Ne $+ ^{208}$Pb and ^{20}Ne $+ ^{90}$Zr, measured at the grazing angles for incident energies of 25 and 30 MeV per nucleon and summed for the various magnetic exposures, are shown in Fig. 2. They have been obtained using the full 1.5° angular acceptance of the spectrometer. The ^{20}Ne
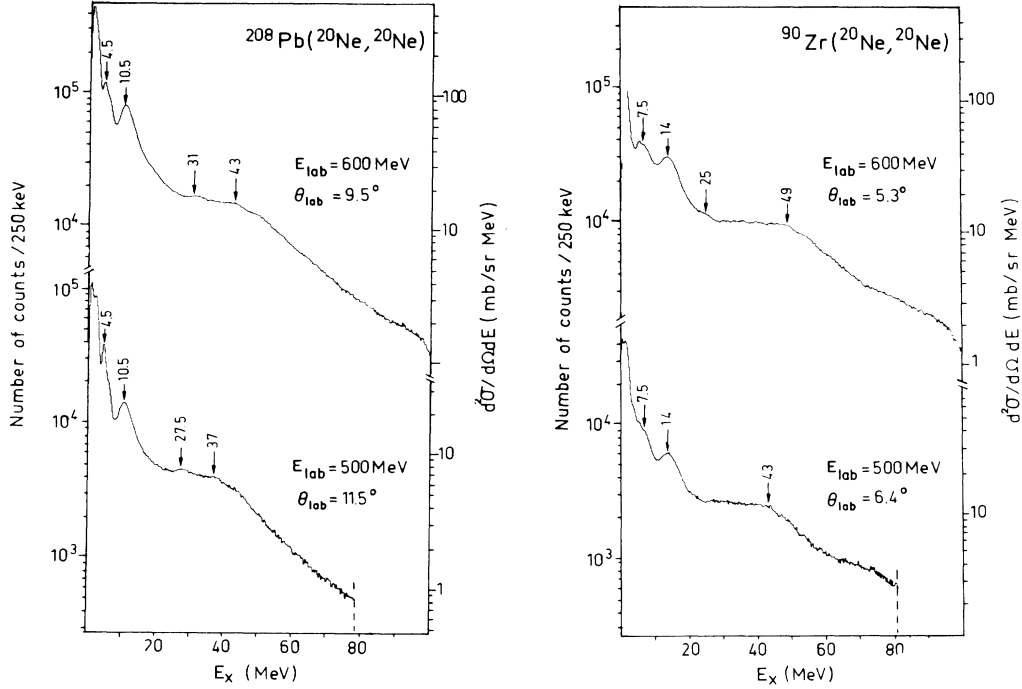

FIG. 1. Typical mass identification spectrum for the neon isotopes (here the elastic events were not counted by the detectors).

FIG. 2. Inelastic scattering spectra at the grazing angles from the reactions ^{20}Ne $+^{208}$Pb (left) and ^{20}Ne $+^{90}$Zr (right) at 500 and 600 MeV incident energies. They were obtained with the full 1.5° angular range of the spectrometer.

$+^{208}$Pb spectra at both incident energies are clearly dominated at low apparent excitation energy by the tail of the elastic peak and a narrow peak located at about 4.5 MeV, which could contain some contribution from the mutual excitation of the 3^- state at 2.61 MeV in ^{208}Pb and the 2^+ state at 1.63 MeV in ^{20}Ne. The large bump observed at 10.5 MeV, with a half-height width of about 4 MeV, can be identified with the well-known giant quadrupole resonance (GQR), which is generally strongly excited in heavy-ion induced inelastic reactions.[1,2] The present excitation energy agrees with the accepted value[9] for the GQR in ^{208}Pb. Known higher-lying giant resonances, such as the giant $E1$ and $E0$ resonances at about 13.5 MeV probably contribute to the observed high excitation energy tail.

In the same way, the ^{20}Ne $+^{90}$Zr spectra (right part of Fig. 2) exhibit a large excitation of the GQR, which is centered at 14 MeV with a tail extending up to about 20 MeV. This also agrees well with the accepted value[9] for the GQR in ^{90}Zr. At lower apparent excitation energies, unresolved levels in ^{90}Zr and possible projectile excitation may contribute to the large bump centered around 7.5 MeV.

The inelastic spectra at higher excitation energies are expected to be dominated by the effect of the three-body continuum. A substantial part of this three-body continuum results from one-nucleon pick-up reactions that excite unbound states of the quasiprojectiles ^{21}Ne and ^{21}Na which then decay by nucleon emission. This transfer-

evaporation process (TEP) will be discussed in Sec. III B. Target excitations at high energy should manifest themselves as small bumps, superimposed on this physical background and located at the same excitation energies in the spectra obtained at the two beam energies $E/A =25$ and 30 MeV. As some small structures are seen in the spectra of Fig. 2, it is necessary to determine if an interpretation in terms of target excitations is consistent with the present data.

A. Search for high-lying excitations of the target nuclei

1. Cross-correlation analysis

Before making a detailed comparison of the high energy structures observed in the spectra at 25 and 30 MeV/nucleon, a cross-correlation analysis will be discussed. This analysis was carried out in order to obtain a global result about the degree of correlation of the weak structures observed in the spectra. They are analyzed as fluctuations around an average cross section, which is defined by the sliding average method:[10,11]

$$\overline{N}_k(E_i) = \frac{1}{2n+1} \sum_{j=i-n}^{i+n} N_k(E_j) , \qquad (1)$$

where $N_k(E_j)$ is the number of counts in the channel E_j of the spectrum k. In the present case, n corresponds to an averaging interval of ± 4 MeV.

The cross-correlation coefficient for two different spectra $N_1(E_i)$ and $N_2(E_i)$ is defined by:[10,11]

$$C_{12} = \left\langle \left[\frac{N_1 - \overline{N}_1}{N_1} \right] \left[\frac{N_2 - \overline{N}_2}{N_2} \right] \right\rangle \Bigg/ \left[\left\langle \left[\frac{N_1 - \overline{N}_1}{N_1} \right]^2 \right\rangle \left\langle \left[\frac{N_2 - \overline{N}_2}{N_2} \right]^2 \right\rangle \right]^{1/2} . \qquad (2)$$

Its possible values are between $+1$ (case of two identical spectra) and -1 (oscillations strictly out of phase), 0 corresponding to noncorrelated spectra.

It is useful to compare this coefficient to those obtained for the same spectra which have been shifted one relative to the other by a number of channels, Δ. The values of the function $C_{12}(\Delta)$ for different pairs of spectra are presented in Fig. 3; they have been calculated for an excitation energy range from 25 to 55 MeV.

The cross-correlation analysis was first carried out for pairs of spectra accumulated at two different settings of the magnetic field ($H1$ and $H2$ in Fig. 3) in order to check the consistency of the measurements. The results are displayed in the upper part of Fig. 3 (for the experiments at 600 MeV, the "$H2$" spectra correspond to the sum of spectra obtained at five neighboring exposures). The strong positive value of C_{12} for unshifted spectra ($\Delta=0$) clearly shows that the main oscillations observed in the spectra do not come from statistical fluctuations or the differential nonlinearity of the detector, and therefore have a physical origin.

The results of this analysis for the total spectra measured at 500 and 600 MeV are shown in the lower part of Fig. 3. For the ^{20}Ne $+^{208}$Pb system, the coefficient C_{12} is strongly negative at $\Delta=0$, which indicates that

FIG. 3. Cross correlation functions $C_{12}(\Delta)$ for the inelastic scattering spectra from the reactions ^{20}Ne $+^{208}$Pb (left) and ^{20}Ne $+^{90}$Zr (right) in the 25 to 55 MeV apparent excitation energy range (see text). The upper part of the figure corresponds to partial spectra at two different magnetic exposures "$H1$" and "$H2$" at each incident energy. The lower part corresponds to the correlation of the total spectra at 500 and 600 MeV.

the structures are anticorrelated. Instead it takes its maximum value when one of the spectra is shifted by about 5 MeV relative to the other. A different result is obtained for the ^{20}Ne $+^{90}$Zr spectra; the correlation function is rather flat with a C_{12} value for unshifted spectra close to zero. These results therefore indicate that a target excitation is not the dominant process for the origin of these bumps in the two systems ^{20}Ne $+^{208}$Pb and ^{20}Ne $+^{90}$Zr.

2. Comparison with previous results

The above conclusions, which result from the application of statistical methods, can also be drawn from a visual comparison of the spectra at 25 and 30 MeV/nucleon. These spectra are presented with appropriate scales in Fig. 4 for ^{90}Zr and Fig. 5 for ^{208}Pb. The average position of the structures which were reported in Refs. 4 and 5, and identified with target excitations, are also indicated above the present spectra for comparison. The rather large error bars on these excitation energies result from the difficulty of accurately determining the centroids of small structures with low statistical accuracy since they depend on the choice of subtracted background.[4]

(a) The ^{20}Ne $+^{90}$Zr data. At $E/A=30$ MeV, the dominant features of the spectrum are the following: a bump centered at 25 MeV with a width of about 4 MeV, a plateau from 28 to 49 MeV, a falloff of the cross section by a factor of about 3 up to an inflection point located at 71 MeV. In this last region, a smooth oscillation can be observed at about 54 MeV. The physical origin of other structures, in particular the weak and narrow ones located on the plateau, could not be firmly established by comparison of partial spectra at different exposures.

Similar features are observed for the spectrum at $E/A=25$ MeV except that they are shifted to lower excitation energies; weak out-of-phase structures are quite as numerous as weak in-phase ones, and moreover their excitation energies do not generally correspond to the ones found in the previous measurements of Refs. 4 and 5, which were mainly performed with ^{40}Ar beams. The only meaningful comparison with previous results is to give an upper limit on cross sections for exciting the same structures. As an example, if one tentatively identifies the very weak structure between 29 and 32 MeV in both spectra with the 29 ± 1.5 MeV "bump" from Refs. 4 and 5, then its cross section at 30 MeV/nucleon would be about 0.7 mb/sr, which is only 1.5% of the one measured for the underlying background.

(b) The ^{20}Ne $+^{208}$Pb data. Some oscillations can be noticed in the region of the spectrum near the sharp fall-off of the cross section between the giant quadrupole resonance and 25 MeV, as can be seen in the left-hand side of Fig. 5. They correspond to about 3% to 4% of the underlying background. However, it is not possible to identify them with high energy resonances in ^{208}Pb, as their position and width are different at $E/A=25$ and
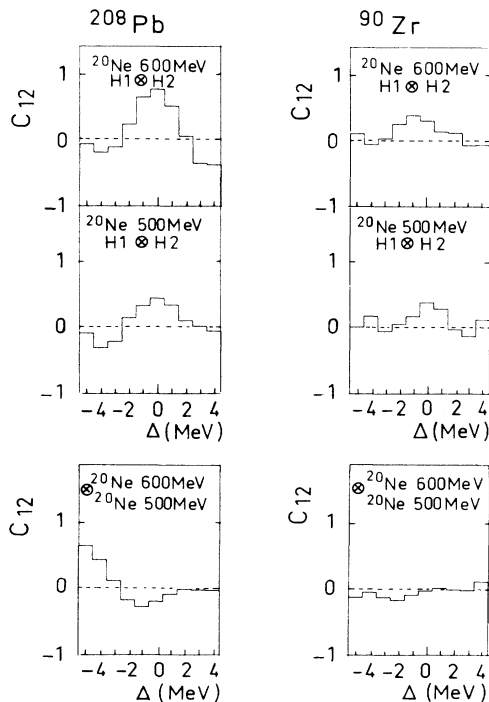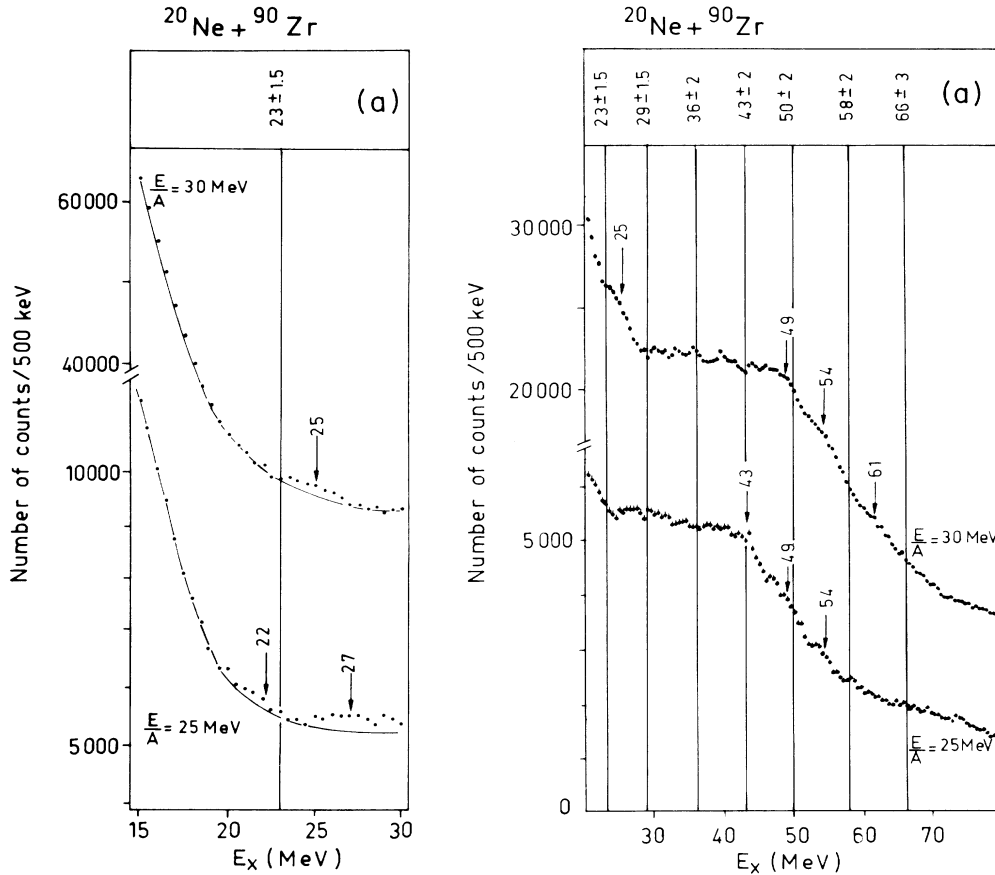
FIG. 4. Comparison of the ^{20}Ne $+^{90}$Zr inelastic scattering spectra at $E/A = 25$ MeV ($\theta_{lab} = 6.4°$) and 30 MeV ($\theta_{lab} = 5.3°$). Two different scales are used for the low excitation energy part (left) and high excitation energy part (right) in order to enhance the weak structures observed in the spectra. The lines under the spectra are to guide the eye. Above the spectra (a), the excitation energies from Refs. 4 and 5 are given for comparison.

30 MeV. In particular a bump is observed at 18.5 MeV apparent excitation energy in the 30 MeV spectrum, but it cannot be firmly identified with the high energy octupole resonance in ^{208}Pb as reported in light ion inelastic scattering[12] since it is not confirmed by the 25 MeV data.

At $E/A = 30$ MeV, the high excitation energy part of the inelastic spectrum (right-hand side of Fig. 4) exhibits two main bumps at 31 and 43 MeV, which stand clearly above the continuum, and a weaker structure at 49 MeV, which is observed as a shoulder in the steeply decreasing background. This spectrum has been compared to those obtained in the previous studies reported in Refs. 3 and 7 for the same system at the same incident energy. Contradictory results were given by these two experiments; the existence of seven bumps between 25 and 80 MeV apparent excitation energies, which was reported in Ref. 3, has not been confirmed in Ref. 7. In fact, in this second experiment, only three small structures at 31, 43, and 50 MeV were observed. However, their origin from nuclear processes was strongly questioned by the authors due to small differential linearity defects in the focal plane counter. The present spec-

trum, which was obtained with much better statistics [about 60 000 counts/MeV at 40 MeV as compared to 100 counts (Ref. 3) and 3000 counts (Ref. 7)], exhibits the same features as observed in Ref. 7 and definitely establishes the existence of these structures.

The evolution of the shape of the inelastic spectrum relative to angle, as observed in the present data at $E/A = 30$ MeV, is shown in Fig. 6. The bumps at 31 and 43 MeV, which are not observed at 7° and 9°, are clearly visible at 9.5° and 10°, whereas they appear to be masked by the large three-body continuum observed in spectra at more backward angles. This enhancement of the relative cross section at the grazing angle is similar to the one reported in Ref. 4 for the high excitation energy structures.

The inelastic spectrum at $E/A = 25$ MeV is presented in the lower part of Fig. 5 for comparison with the 30 MeV/nucleon data. Two structures at 27.5 and 37 MeV and a weaker one at 44 MeV are observed. They are quite out of phase with those present in the spectrum at $E/A = 30$ MeV. This fact had been illustrated before in Fig. 3, for which the corresponding cross-correlation coefficient for unshifted spectra ($\Delta = 0$) have a negative
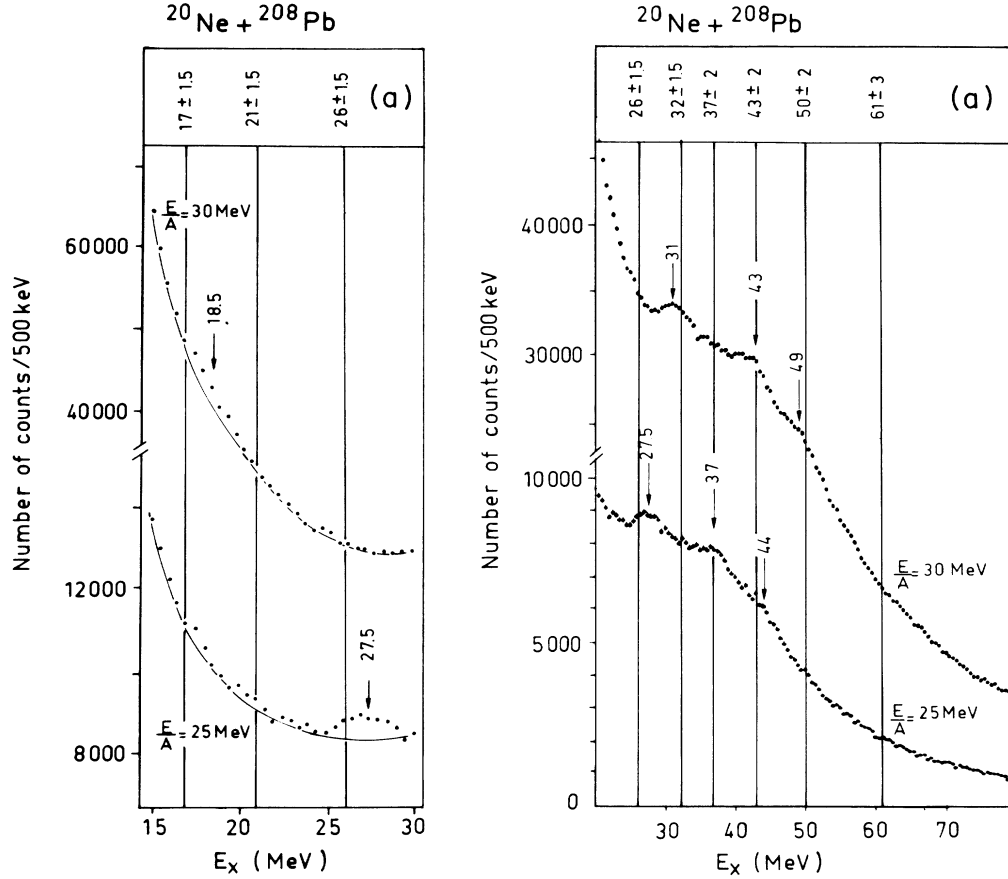
^{20}Ne + ^{208}Pb

^{20}Ne + ^{208}Pb

(a)

(a)

17 ± 1.5   21 ± 1.5   26 ± 1.5

26 ± 1.5   32 ± 1.5   37 ± 2   43 ± 2   50 ± 2   61 ± 3

Number of counts/500 keV

Number of counts/500 keV

$\frac{E}{A}$ = 30 MeV

18.5

60000

40000

40000

30000

31

43

12000

49

27.5

$\frac{E}{A}$ = 25 MeV

10000

27.5

37

8000

44

5000

$\frac{E}{A}$ = 30 MeV

$\frac{E}{A}$ = 25 MeV

0

15   20   25   30

30   40   50   60   70

E_x (MeV)

E_x (MeV)

FIG. 5. Same as Fig. 4 for the ^{20}Ne + ^{208}Pb reaction at $E/A = 25$ MeV ($\theta_{lab} = 11.5°$) and 30 MeV ($\theta_{lab} = 9.5°$).

value. Thus, the assumption that the origin of these structures could be target excitations is in complete contradiction with the present results.

However, as these bumps have a large cross section (about 4 mb/sr at $E/A = 30$ MeV and 3 mb/sr at $E/A = 25$ MeV for the two strongest ones), it is possible that target excitations with smaller cross sections are hidden by these larger bumps. In such a case, the corresponding excitation cross section can be estimated to be lower than about 0.5 mb/sr in the present reaction at $E/A = 30$ MeV.

B. Transfer-evaporation processes (TEP) in the ^{20}Ne inelastic spectra

Since the apparent excitation energies of the high-lying structures are observed to depend on the incident energy, one has to consider the possibility that they are related to transfer-evaporation processes (TEP), which are expected to account for a large part of the noninelastic background. A strong excitation of a discrete unbound state in the quasiprojectile is in fact expected to give rise to shoulders superimposed on the TEP bump, which is due to the other excited unbound states. An enhancement of these shoulders into well-developed bumps can even occur if the angular distribution of the emitted nucleon is anisotropic.[13,14] Such a case was first

clearly shown for a heavy ion induced reaction in a study of the ^{16}O + ^{208}Pb inelastic scattering.[2]

The kinematical characteristics of the contribution of TEP to inelastic scattering spectra have been reported in Refs. 13 and 14. If the quasiprojectile after being excited in an unbound state by a one-nucleon pick up, emits a nucleon with a center-of-mass energy ϵ_n, it will finally be detected in the inelastic spectrum in a well-defined range of apparent excitation energies. The extreme of this contribution will be located at

$$E_x \simeq \frac{E_I}{A+1} + S_N(T) + E^* + \epsilon_n \pm \Delta \ , \tag{3}$$

with

$$\Delta = \frac{2(A_T + A)}{A_T} \left[\frac{E_I \epsilon_n}{A+1} \right]^{1/2} , \tag{4}$$

where E_I is the incident energy, A and A_T are the masses of the projectile and target, $S_N(T)$ is the separation energy of the nucleon in the target nucleus, and E^* is the excitation energy of the residual fragment.

If one then assumes that the relative pick-up cross sections to various ^{21}Ne and ^{21}Na unbound states are nearly the same at both incident energies, it is possible to deduce the shape of the TEP contribution in the inelastic spectrum at 25 MeV/nucleon from the one observed
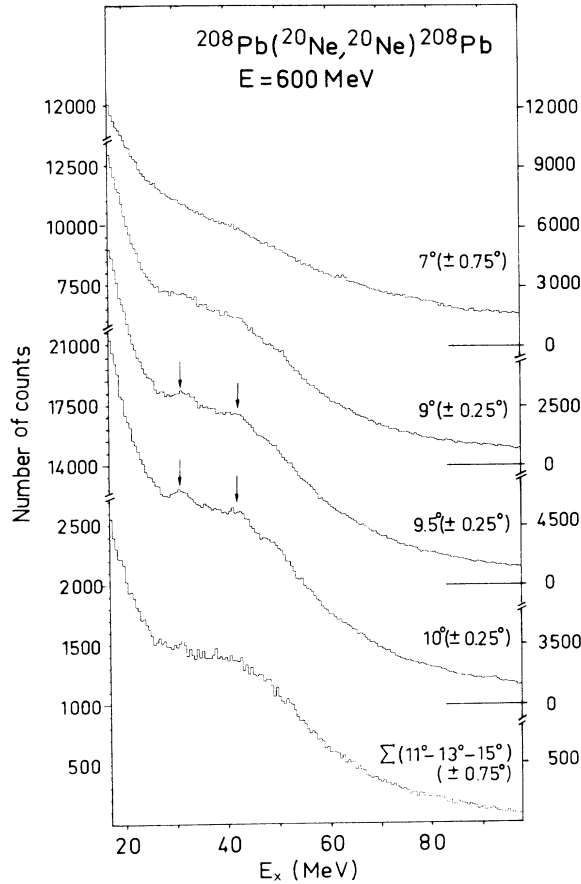
FIG. 6. Inelastic scattering spectra from the ^{20}Ne $+^{208}$Pb reaction at $E/A = 30$ MeV, at different laboratory angles. The arrows indicate the positions of the structures at apparent excitation energies of 31 and 43 MeV.

TEP contribution to the inelastic spectrum, it would be necessary to know the relative excitation of each unbound state in ^{21}Ne and ^{21}Na for every system under investigation. In the present case, these data are unknown, and only some remarks can be made.

(i) In a study of the ^{20}Ne $+^{58}$Ni system at 290 MeV incident energy,[14] it was shown that discrete unbound states in ^{21}Ne were excited with the emission of two groups of neutrons with $\epsilon_n = 0.4$ MeV and 2 MeV.

(ii) Similar data do not exist for ^{21}Na, but the proton emission threshold is very low (2.4 MeV), and several discrete unbound states are good candidates to be appreciably excited. This would give rise to subsequent proton emission and thus to structures in the TEP bump. For example, the lowest lying unbound state ($J^\pi = \frac{1}{2}^-$) is at 2.8 MeV, and it is expected to decay by emission of a 0.4 MeV proton rather than by gamma emission, in view of the relative partial lifetime predicted for these two processes.

(iii) The relative importance of the ^{21}Na contribution to the TEP bump in the inelastic spectra for ^{208}Pb and ^{90}Zr can be roughly estimated by considering the ratio of cross sections measured for the production of bound
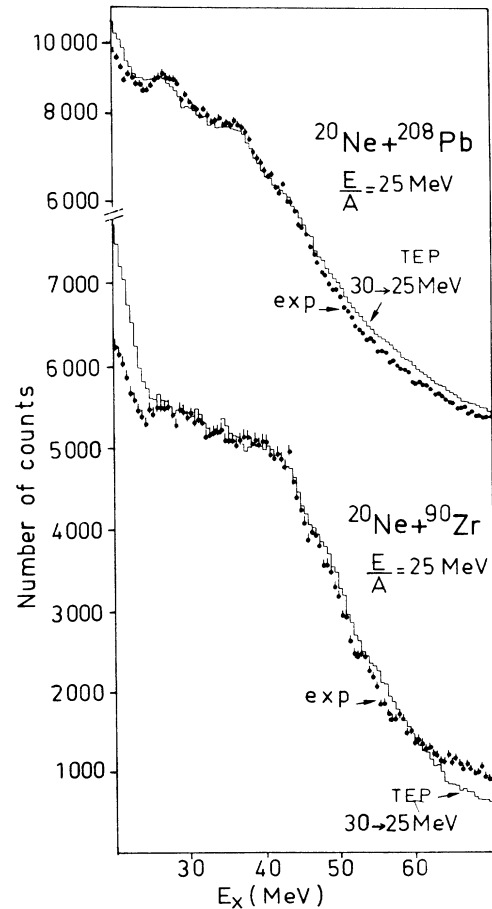
at 30 MeV/nucleon. This can be done by shifting and contracting it properly, according to Eqs. (3) and (4). Without any background subtraction the spectra $E/A = 30$ MeV for ^{208}Pb and ^{90}Zr have been transformed into "theoretical spectra" at $E/A = 25$ MeV. For this purpose the code TRAPUBU,[15] which is based on the kinematics of TEP, was used. The resulting calculated spectra, multiplied by an appropriate normalization factor, are presented as solid lines in Fig. 7 and compared to the actual spectra at that energy.

With the exception of the low- and high-energy parts of the spectra, which are irrelevant to the TEP, quite good agreement is observed between the experimental and transformed spectra, which shows that the cross section in this region is in fact mainly due to this process. This is also the case for ^{90}Zr (lower part of Fig. 7), for which the shapes of both spectra are very similar. Moreover, in the ^{20}Ne $+^{208}$Pb system (upper part of Fig. 7), it is quite remarkable that the two bumps at 27.5 and 37 MeV observed at $E/A = 25$ MeV appear as a kinematical transformation of those at 31 and 43 MeV in the $E/A = 30$ MeV spectrum, thus making evident that they originate from TEP.

In order to obtain a quantitative interpretation of the

FIG. 7. Comparison of the experimental inelastic spectra at $E/A = 25$ MeV (points with error bars) with the calculated shapes (solid lines) predicted from the $E/A = 30$ MeV data using the TEP kinematical relations (see text).

^{21}Ne and ^{21}Na in the present experiment. At $E/A = 30$ MeV at the grazing angle, its value for apparent excitation energies below 10 MeV is about 18 for ^{208}Pb and 5 for ^{90}Zr. If one assumes a similar behavior for unbound states, this suggests that the contribution of proton pick up to the TEP could be about three to four times more important for ^{90}Zr than for ^{208}Pb targets. Another comment can also be made on these large ratios of ^{21}Ne to ^{21}Na production cross sections. They are probably partly due to the different particle thresholds for these two nuclei (6.8 and 2.4 MeV, respectively), since the excitation of a ^{21}Na state located between these two energies would give rise to a TEP contribution in the inelastic ^{20}Ne spectrum, unlike the mirror state decaying by γ decay. Therefore, the tentative conclusion is that TEP from proton pick-up reactions may be not negligible, particularly for ^{90}Zr.

The positions of the edges of discrete TEP contributions in the inelastic spectra have been calculated for various possible ^{21}Ne and ^{21}Na unbound states with Eq. (3) under the assumption that the quasitarget is left in its ground state. These calculated positions are indicated by arrows in Fig. 8 for the four spectra in the case of the emission of 0.4 and 2 MeV neutrons and 0.4 MeV protons, energies chosen on the basis of the above discussion.

A tentative interpretation of the main oscillations which are observed in the spectra could then be as follows. In the ^{20}Ne $+^{208}$Pb system, the double bumps at 27.5–37 MeV and 31–43 MeV could correspond to the decay of an unbound state in ^{21}Ne which emits a neutron of 0.4 MeV since the edges of its calculated contribution correspond fairly well to the edges observed experimentally. This agreement is quite satisfactory when one considers that the positions of the arrows do not account for possible additional mutual excitation of ^{207}Pb at energy E^*, which would shift the position of the high-energy arrow to the right. This effect, and also those from experimental energy resolution and angular distribution effects, should be included for a quantitative reproduction of the experimental shape.

The corresponding double bump in ^{90}Zr was not observed. This could be because the excitation cross section is lower than in ^{208}Pb. On the other hand, if an unbound low-lying ^{21}Na level was strongly excited in the ^{20}Ne $+^{90}$Zr system, the proton and neutron double bumps would be out of phase (cf. the arrows of Fig. 8), thus giving rise to a rather flat continuum, which would appear similar to that experimentally observed.

One can also attempt to identify the effect of the ^{21}Ne decay into a 2 MeV neutron as shown in Ref. 14. It could explain the shoulder at 49 MeV in the ^{20}Ne $+^{208}$Pb spectrum at $E/A = 30$ MeV (43 MeV at 25 MeV/nucleon). The corresponding low-energy shoulder can not be clearly distinguished in the tail of the giant quadrupole resonance. For the ^{20}Ne $+^{90}$Zr spectra, this emission of 2 MeV neutrons could explain the low-energy bump at, respectively, 22 and 25 MeV, in the spectra at $E/A = 25$ and 30 MeV, and the main oscillation in the fall of the TEP bump, located at 54 and 61 MeV, respectively.
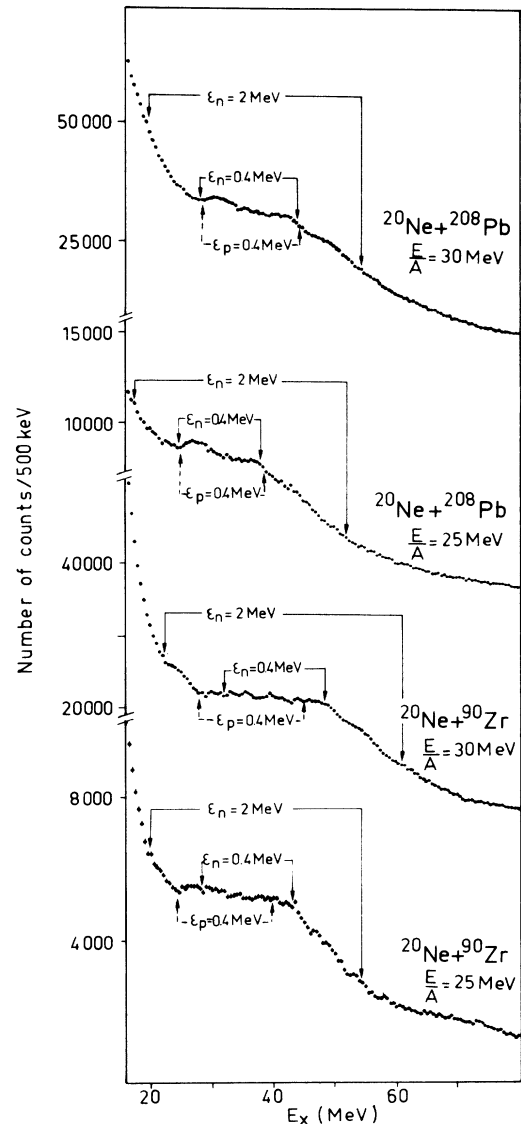

FIG. 8. Inelastic spectra at grazing angles from the ^{20}Ne $+^{208}$Pb and ^{20}Ne $+^{90}$Zr reactions at $E/A = 30$ and 25 MeV. The edges of the TEP contribution from discrete unbound states in ^{21}Ne which emit neutrons with energies ϵ_n of 0.4 and 2 MeV (see text) are indicated with arrows. The possible contribution of a ^{21}Na state which emits a proton with energy ϵ_p of 0.4 MeV is also shown for comparison.

IV. CONCLUSION

Structures at high apparent excitation energies have been clearly seen in the inelastic scattering spectra measured at grazing angles for ^{20}Ne $+^{90}$Zr and ^{20}Ne $+^{208}$Pb at $E/A = 25$ and 30 MeV. However, their shift in apparent excitation energy with incident beam energy rules out the possibility that they originate from target excitation and the related interpretation in terms of multiphonon excitations as proposed in Refs. 4 and 5. Only an upper limit for the corresponding excitation cross section could be found in the present study. On the other

hand, a transfer-evaporation process nicely accounts for the existence of these high-lying structures. Therefore, the conclusions of Refs. 3–5 about the excitation of high energy resonances in ^{90}Zr and ^{208}Pb should be carefully checked, in particular by ruling out the possibility of discrete TEP effects in the ^{40}Ar inelastic scattering spectra. There have been now three studies using ^{17}O, ^{20}Ne, and ^{32}S probes (Refs. 7 and 8 and present work) which do not observe these high lying target excitations reported in Refs. 3–5. It is clear that any further search for multiphonon excitations implies the minimization of the contribution from three-body processes in the inelastic spectra by an appropriate choice of the projectile. Furthermore, the use of coincidence techniques may

help to disentangle the target excitations from other underlying processes.

*On leave from Institut de Physique Nucleaire, 91406 Orsay Cedex, France.

†Present address: Department of Physics, University of Groningen, 9718CM Groningen, The Netherlands.

[1] M. Buenerd, D. Lebrun, J. Chauvin, Y. Gaillard, P. Martin, G. Perrin, and P. de Saintignon, Phys. Rev. Lett. **40**, 1482 (1978).

[2] T. P. Sjoreen, F. E. Bertrand, R. L. Auble, E. E. Gross, D. J. Horen, D. Shapira, and D. B. Wright, Phys. Rev. C **29**, 1370 (1984).

[3] Ph. Chomaz, N. Frascaria, Y. Blumenfeld, J. P. Garron, J. C. Jacmart, J. C. Roynette, W. Bohne, A. Gamp, W. Von Oertzen, M. Buenerd, D. Lebrun, and P. Martin, Z. Phys. A **318**, 41 (1984).

[4] N. Frascaria, XXIV International Winter Meeting on Nuclear Physics, Bormio, 1986 (unpublished), p. 71, and references therein.

[5] N. Frascaria, Y. Blumenfeld, Ph. Chomaz, J. P. Garron, J. C. Jacmart, J. C. Roynette, T. Suomijarvi, and W. Mittig. Report No. IPNO-DRE-87-10; Nucl. Phys. A (in press).

[6] Ph. Chomaz and D. Vautherin, Phys. Lett. **139B**, 244 (1984); Ph. Chomaz, These, de 3ème Cycle, Université Paris–Sud,

1984 (Report No. IPNO-T-84-01).

[7] M. Buenerd, J. Chauvin, G. Duhamel, J. Y. Hostachy, D. Lebrun, P. Martin, P. O. Pellegrin, G. Perrin, and P. de Saintignon, Phys. Lett. **167B**, 379 (1986).

[8] F. E. Bertrand, R. O. Sayer, R. L. Auble, M. Beckerman, J. L. Blankenship, B. L. Burks, M. A. G. Fernandes, C. W. Glover, E. E. Gross, D. J. Horen, J. Gomez del Campo, D. Shapira, and H. P. Morsch, Phys. Rev. C **35**, 111 (1987).

[9] F. E. Bertrand, International Conference on Nuclear Physics, Berkeley, 1980 [Nucl. Phys. **A354**, 129 (1981)], and references therein.

[10] A. Richter, in *Nuclear Spectroscopy and Reactions,* edited by J. Cerny (Academic, New York, 1974).

[11] T. Suömijarvi, private communication.

[12] H. P. Morsch, D. Cha, and J. Wambach, Phys. Rev. C **31**, 1715 (1985), and references therein.

[13] Y. Blumenfeld, J. C. Roynette, Ph. Chomaz, N. Frascaria, J. P. Garron, and J. C. Jacmart, Nucl. Phys. **A445**, 151 (1985).

[14] H. G. Bohlen, H. Ossenbrink, H. Lettau, and W. Von Oertzen, Z. Phys. A **320**, 237 (1985).

[15] Ph. Chomaz and J. C. Roynette, private communication.